Binding of Unfused Aromatic Cations to DNA. The Influence of Molecular Twist on Intercalation

W. David Wilson,*,† Lucjan Strekowski,*,† Farial A. Tanious,† Rebecca A. Watson,† Jerzy L. Mokrosz,† Alewtina Strekowska,† Gordon D. Webster,‡ and Stephen Neidle*,‡

Contribution from the Department of Chemistry, Georgia State University, Atlanta, Georgia 30303-3083, and CRC Biomolecular Structure Unit, The Institute of Cancer Research, Sutton, Surrey SM2 5PX, U.K. *Received April 6, 1988*

Abstract: A new type of intercalator, **1**, and its nonintercalating analogue, **2**, are both twisted about the torsional bonds joining the aromatic rings. Spectroscopic methods and MM2 calculations indicate that the twist for **2** is significantly greater than for **1** (48° versus 25° from MM2) in solution. X-ray crystallographic analysis indicates that the torsional angles are 10° and 19° for the two phenyl-pyrimidine plane intersections in **1**. The DNA binding constant for **1** is similar to those for other strong intercalators, and viscometric, flow dichroism, and NMR experiments (nonexchangeable protons of **1**, imino proton, and ^{31}P spectra of DNA in the complex) indicate that **1** binds to DNA by intercalation. The binding constant for **2** is less than that for **1**, and viscosity, dichroism, and NMR experiments demonstrate that **2** does not intercalate. The structure of **1**, with a twisted aromatic system and terminal basic functions, is analogous to many groove-binding compounds, and it is, thus, unexpected that **1** forms a strong intercalation complex with DNA. The twist of **1** may complement or enhance the intrinsic propeller twist of DNA base pairs to allow intercalation. Molecular mechanics methods located two potential low-energy intercalation conformations of **1** at the CG intercalation site of the hexamer d(TACGTA). A straddling model with one side chain of **1** in each groove of DNA was rejected on kinetic grounds. The other low-energy conformation, and the one that agrees best with the experimental results, has both cationic substituents of **1** in the major groove with partial stacking of the three unfused rings with the base pairs at the intercalation site. A similar binding geometry of **1** in the minor groove was not feasible due to numerous unfavorable close contacts between the cationic groups and the DNA atoms in the minor groove. With **2** the intrinsic molecular twist is larger, and it does not form an intercalation complex. The bleomycin amplification activity of **1** is significantly greater than that for **2**.

It has been generally observed that unfused aromatic ring compounds with terminal basic functions bind to DNA in one of the grooves while fused ring aromatic cations bind most strongly to DNA in an intercalation complex.[1-7] Some unfused ring intercalators, particularly bicyclic monocations, have been identified,[8,9] and it has been speculated that the bithiazole portion of bleomycin intercalates.[8,10] In addition, fused ring compounds can bind to the exterior of the DNA helix in a nonspecific, stacked complex, which is stabilized by the DNA phosphate charges and is generally 1-2 orders of magnitude less strongly bound than the favored intercalation complex.[1,2,11] Presumably because of their intrinsic twist and superior groove interactions, it has not been demonstrated that classical groove-binding molecules such as netropsin and distamycin have a competing intercalation binding mode. On the other hand, the base pairs of DNA have sequence-dependent local variations in geometry, which can include significant base-pair propellar twist.[12,13] It would seem then that a certain amount of intrinsic twist could be accommodated in an intercalation ring system and, in fact, could be quite favorable if it appropriately matched the conformational requirements of base-pair twist in an intercalation complex.

There is a class of unfused aromatic cations that bind with and amplify the degradation of DNA by bleomycin and its analogues.[9,14] As part of a study of the mechanism by which these compounds amplify the bleomycin-catalyzed digestion of DNA,[9] we have begun the synthesis and analysis of DNA interaction properties of a series of unfused aromatic cations that have been designed to exhibit quite different properties in their DNA complexes. In this paper we report on the interaction of the unfused tricyclic dications **1** and **2** (structures in Figure 3) with DNA. These compounds were designed as the first of a series of tricyclic cations, which have a variation in twist in the unfused aromatic ring system, with the goals of creating sets of intercalators with variations in intrinsic twist and molecules, which switch between intercalation and groove-binding behavior as a result of variations in molecular twist. We report here that the interaction of the closely related compounds **1** and **2** with DNA is strikingly different, with **1** binding to DNA by intercalation and **2** binding in a nonintercalation mode. The structure of **1**, with a nonplanar

Scheme I

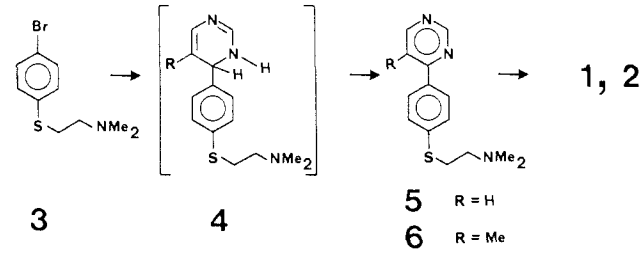

† Georgia State University.
‡ The Institute of Cancer Research.

(1) Waring, M. In *The Molecular Basis of Antibiotic Action*; Gale, F. F., Cundiffe, E., Reynolds, R. E., Richmond, M. H., Waring, M. J., Eds.; Wiley: London, 1981; pp 314-333.
(2) Wilson, W. D.; Jones, R. L. *Adv. Pharmacol. Chemother.* **1981**, *18*, 177-222.
(3) Berman, H. M.; Young, P. R. *Annu. Rev. Biophys. Bioeng.* **1981**, *10*, 87-114.
(4) (a) Neidle, S.; Abraham, Z. *CRC Crit. Rev. Biochem.* **1984**, *17*, 73-121. (b) Neidle, S.; Pearl, L. H.; Skelly, J. V. *Biochem. J.* **1987**, *243*, 1-13.
(5) Braithwaite, A. W.; Baguley, B. C. *Biochemistry* **1980**, *19*, 1101-1106.
(6) Dervan, P. B. *Science (Washington, D.C.)* **1986**, *232*, 464-471.
(7) Zimmer, C.; Wahnert, U. *Prog. Biophys. Mol. Biol.* **1986**, *47*, 31-112.
(8) (a) Sakai, T. T.; Riordan, J. M.; Glickson, J. D. *Biochemistry* **1982**, *21*, 805-816. (b) Riordan, J. M.; Sakai, T. T. *J. Med. Chem.* **1983**, *26*, 884-891. (c) Sakai, T. T.; Riordan, J. M.; Kumar, N. G.; Haberle, F. J.; Elgavish, G. A.; Glickson, J. D. *J. Biomol. Struct. Dyn.* **1983**, *1*, 809-827. (d) Fisher, L. M.; Kuroda, R.; Sakai, T. T. *Biochemistry* **1985**, *24*, 3199-3207.
(9) (a) Strekowski, L.; Chandrasekaran, S.; Wang, Y. H.; Edwards, W. D.; Wilson, W. D. *J. Med. Chem.* **1986**, *29*, 1311-1315. (b) Strekowski, L.; Strekowska, A.; Watson, R. A.; Tanious, F. A.; Nguyen, L. J.; Wilson, W. D. *J. Med. Chem.* **1987**, *30*, 1415-1420. (c) Strekowski, L.; Tanious, F. A.; Chandrasekanan, S.; Watson, R. A.; Wilson, W. D. *Tetrahedron Lett.* **1986**, *27*, 6045-6048. (d) Strekowski, L.; Watson, R. A.; Wilson, W. D. *Nucleic Acids Res.* **1987**, *15*, 8511-8519. (e) Strekowski, L.; Mokrosz, J. L.; Tanious, F. A.; Watson, R. A.; Harden, D.; Mokrosz, M.; Edwards, W. D.; Wilson, W. D. *J. Med. Chem.* **1988**, *31*, 1231-1239. (f) Strekowski, L.; Wilson, W. D.; Mokrosz, J. L.; Strekowska, A.; Koziol, A. E.; Palenik, G. J. *Anti-Cancer Drug Des.* **1988**, *2*, 387-398. (g) Strekowski, L.; Mokrosz, M.; Mokrosz, J. L.; Strekowska, A.; Allison, S. A.; Wilson, W. D. *Anti-Cancer Drug Des.* **1988**, *3*, 79-89.

0002-7863/88/1510-8292$01.50/0

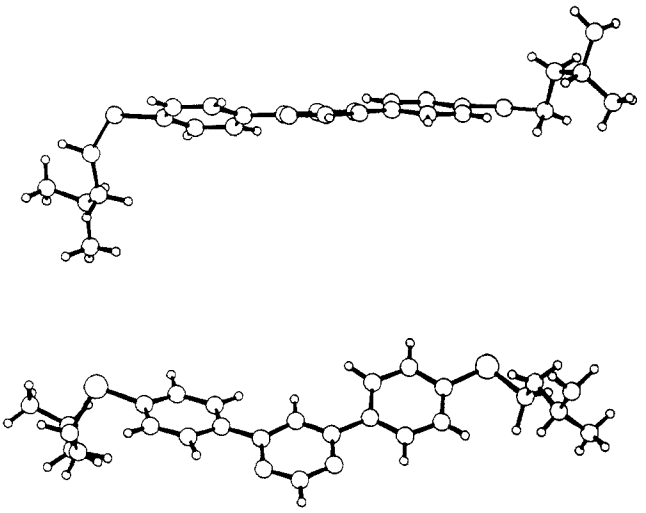

Figure 1. Views of the crystallographic molecular structure for **1**.

ring system in its equilibrium conformation and terminal basic functions, is more analogous to classical groove-binding compounds, such as netropsin and distamycin, than to intercalators.[1-7,15] The fact that it forms a strong intercalation complex with DNA is quite unexpected.

Results

Synthesis of 1 and 2. A lithium reagent obtained from **3** was reacted with pyrimidine or 5-methylpyrimidine to produce the respective dihydropyrimidines (**4**), which, without isolation, were aromatized to **5** or **6** by treatment with DDQ (Scheme I). The addition reactions of the same lithium reagent with **5** or **6** were followed by treatment with DDQ of the intermediate dihydropyrimidines to give **1** or **2**, respectively.

Structures of 1 and 2. MM2 calculations[16] predicted minimum energy conformations of **1** and **2** with the phenyl rings twisted by 25° and 48°, respectively, with respect to the central pyrimidine ring (calculations were done on the system consisting of the central pyrimidine ring and phenyl substituents). The significantly larger twist of **2** relative that to **1** is also supported by absorption and NMR spectral results on the two compounds (vide infra). Calculations involving rotation of one of the phenyl rings about the phenyl–pyrimidine bond indicated a barrier to formation of a planar conformation (of the two rings) of approximately 0.5 kcal/mol for **1**. As expected, the barriers to formation of a planar structure (for two rings) for **2** is much larger but can be reduced to approximately 4 kcal/mol by allowing the methyl group to reoptimize its conformation in the structure with two coplanar rings. Locking the three rings of **2** into a planar conformation and allowing the remainder of the molecule to obtain the minimum energy conformation results in a structure that is over 9 kcal/mol higher in energy than the fully optimized conformation. With **1**, a similar optimized planar conformation is predicted to be approximately 0.5 kcal/mol above the energy for the fully energy-minimized conformation.

We have obtained diffraction quality crystals of **1** as the HBr salt, and the structure has been determined by X-ray crystallography. The molecular structure is shown in Figure 1, and positional parameters and molecular geometries are given in Table I. Bond distances and angles are in general unexceptional. The two S–C bond lengths are 1.756 (6) and 1.796 (6) Å. The three rings are twisted in a helical manner with respect to each other. The phenyl ring on the left side of the structure shown in Figure 1 is inclined to the pyrimidine ring by 19.5 (5)° whereas the phenyl ring on the right side of the figure and the pyrimidine are at an angle of 9.8 (5)°. In spite of crystal-packing forces, the observed twist is only slightly less than that predicted by the molecular mechanics calculations. It is noteworthy that the valence angles at atoms C1′, C1″, C4, and C6 are all increased (values of 123.0 (5)°, 122.0 (4)°, 123.5 (5)°, and 123.1 (4)°), indicating that the steric strain induced by the close proximity of three hydrogen atoms in the planar conformation of the three rings has been relieved in part by the observed twist and in part by the observed deformations of valence angles from their ideal sp^2-hybridization values. The fact that the halves of the molecule have distinct twists is indicative of some softness in these two torsion angles. Presumably, the lack of hydrogen atoms attached to the pyrimidine nitrogens of the central ring contributes to the relative planarity of **1**. The two trans-oriented cationic side groups adopt distinct conformations, reflecting their flexibility. Thus, the specific conformation found in the crystal is a consequence of packing and

Table I. Positional Parameters and Their Estimated Standard Deviations for **1**[a]

atom	*x*	*y*	*z*	*B*, Å
Br1	0.6517 (1)	0.17467 (6)	0.36677 (4)	4.53 (1)
Br2	0.1591 (1)	0.67838 (6)	0.38288 (4)	4.46 (1)
S1	0.2989 (2)	1.00221 (1)	0.15962 (8)	3.76 (3)
S2	−1.1494 (2)	0.7257 (1)	−0.23124 (7)	3.38 (3)
N1	−0.6151 (7)	0.5786 (4)	0.0794 (2)	3.10 (9)
N2	−0.35889 (7)	0.6305 (4)	0.1516 (2)	3.4 (1)
N3	−0.8761 (7)	0.6060 (4)	−0.3709 (3)	3.4 (1)
N4	0.3599 (9)	0.9083 (5)	0.3778 (3)	5.1 (1)
C1	−0.0535 (9)	0.7549 (5)	0.1756 (3)	3.3 (1)
C2	0.0956 (9)	0.8172 (5)	0.1909 (3)	3.6 (1)
C3	−0.7230 (8)	0.6798 (4)	−0.0357 (3)	2.6 (1)
C4	−0.1850 (8)	0.7892 (4)	0.1172 (3)	2.5 (1)
C5	−0.3392 (8)	0.7182 (4)	0.1013 (3)	2.7 (1)
C6	−0.6724 (8)	0.7402 (5)	−0.1011 (3)	3.1 (1)
C7	0.1101 (8)	0.9182 (4)	0.1492 (3)	2.8 (1)
C8	−0.1729 (8)	0.8923 (5)	0.0759 (3)	3.0 (1)
C9	−0.4563 (8)	0.7384 (4)	0.0397 (3)	2.9 (1)
C10	−0.0271 (9)	0.9557 (5)	0.0921 (3)	3.4 (1)
C11	−0.4951 (9)	0.5670 (5)	0.1365 (3)	3.6 (1)
C12	−1.0263 (8)	0.6405 (5)	−0.0931 (3)	3.1 (1)
C13	−0.9758 (8)	0.7020 (4)	−0.1575 (3)	2.8 (1)
C14	−0.7968 (9)	0.7508 (5)	−0.1613 (3)	3.4 (1)
C15	−0.9034 (8)	0.6289 (5)	−0.0330 (3)	2.8 (1)
C16	−0.5945 (8)	0.6661 (4)	0.0291 (3)	2.8 (1)
C17	−1.069 (1)	0.6423 (6)	−0.4159 (3)	4.2 (1)
C18	−0.908 (1)	0.5336 (5)	−0.3019 (3)	4.1 (1)
C19	0.2934 (9)	0.9766 (5)	0.3079 (3)	3.3 (1)
C20	0.592 (1)	0.8647 (6)	0.3878 (4)	5.6 (2)
C21	0.430 (1)	0.9375 (6)	0.2417 (3)	4.1 (1)
C22	0.240 (1)	0.9679 (7)	0.4397 (3)	5.4 (2)
C23	−0.683 (1)	0.5431 (7)	−0.4146 (5)	5.9 (2)
C24	−1.114 (1)	0.5786 (5)	−0.2577 (3)	3.9 (1)

[a] Anisotropically refined atoms are given in the form of the isotropic equivalent thermal parameter defined as the following: $^4/_3[a^2B(1,1) + b^2(B(2,2) + c^2B(3,3) + ab(\cos\gamma)B(1,2) + ac(\cos\beta)B(1,3) + bc(\cos\alpha)B(2,3)]$.

(10) (a) Povirk, L. F.; Hogan, M.; Dattagupta, N. *Biochemistry* **1979**, *18*, 96–101. (b) Lin, S. Y.; Grollman, A. P. *Biochemistry* **1981**, *20*, 7589–7598. (c) Henichant, J. P.; Bernier, J. L.; Helbecque, N.; Houssin, R. *Nucleic Acids Res.* **1985**, *13*, 6703–6717. (d) Miller, K. J.; Lauer, M.; Caloccia, W. *Biopolymers* **1985**, *24*, 913–924.

(11) Peacocke, A. R.; Skerrett, J. N. H. *Trans. Faraday Soc.* **1956**, *52*, 261–279.

(12) (a) Calladine, C. R. *J. Mol. Biol.* **1982**, *161*, 343–352. (b) Dickerson, R. E. *J. Mol. Biol.* **1983**, *166*, 419–441 and references therein.

(13) (a) Tung, C. S.; Harvey, S. C. *J. Biol. Chem.* **1986**, *261*, 3700–3709. (b) Tung, C. S.; Harvey, S. C. *Nucleic Acids Res.* **1986**, *14*, 381–387.

(14) (a) For a review, see: Brown, D. J.; Grigg, G. W. *Med. Res. Rev.* **1982**, *2*, 193. (b) Aliano, A. N.; Allen, T. E.; Brown, D. J.; Cowden, W. B.; Grigg, G. W.; Kavulak, D.; Lan, S.-B. *Aust. J. Chem.* **1984**, *37*, 2385. (c) Allen, T. E.; Brown, D. J.; Cowden, W. B.; Grigg, G. W.; Hart, N. K.; Lamberton, J. A.; Lane, A. *J. Antibiot.* **1984**, *37*, 376 and references therein. (d) Grigg, G. W.; Gero, A. V.; Sasse, W. H.; Sleigh, M. J. *Nucleic Acids Res.* **1984**, *12*, 9083.

(15) (a) Berman, H. M.; Neidle, S.; Zimmer, C.; Thrum, H. *Biochem. Biophys. Acta* **1979**, *561*, 124–131. (b) Kopka, M. L.; Yoon, C.; Goodsell, D.; Pjura, P.; Dickerson, R. E. *J. Mol. Biol.* **1985**, *183*, 553–563.

(16) (a) Burket, U.; Allinger, N. L. *Molecular Mechanics*; American Chemical Society: Washington, DC, 1982. (b) Osawa, E.; Musso, H. "Applications of Molecular Mechanics Calculations in Organic Chemistry"; in *Topics in Stereochemistry*; Allinger, N. L., Eliel, E. L., Wilen, S. H., Eds.; Wiley: New York, 1982; p 117. Molecular mechanics calculations were carried out with version 2.0 of the MACROMODEL program supplied by Professor C. Still, Columbia University.

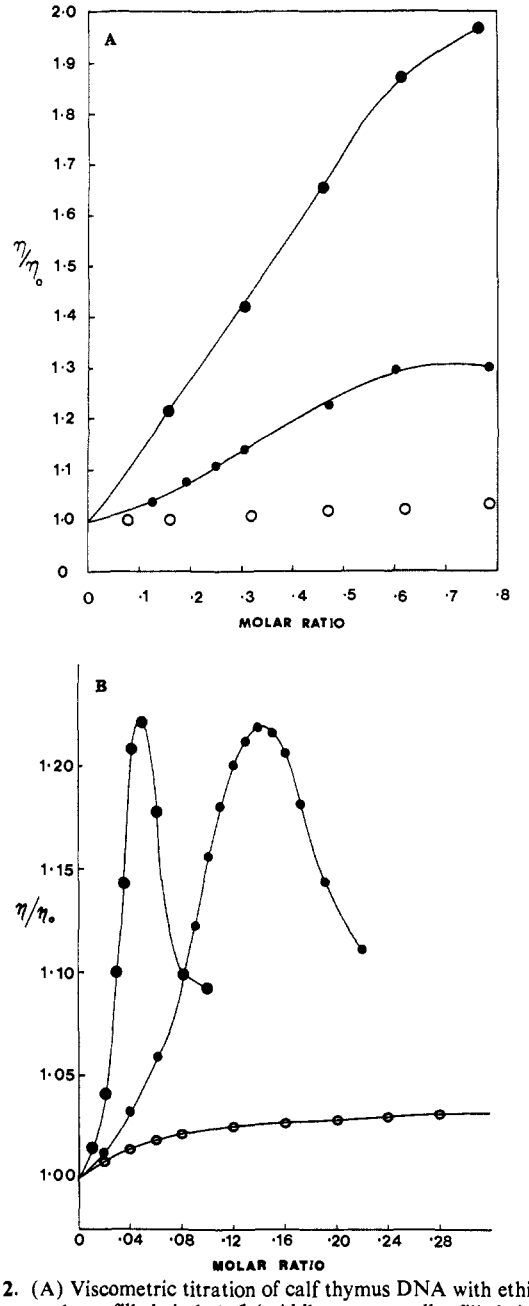

Figure 2. (A) Viscometric titration of calf thymus DNA with ethidium (upper curve, large filled circles), **1** (middle curve, smaller filled circles), and **2** (lower curve, open circles). Titrations were performed in PIPES buffer at 30 °C with sonicated DNA of 800 base pairs of average length. The reduced specific viscosity ratio is plotted versus the molar ratio of compound to DNA base pairs. (B) Viscometric titrations of closed circular pBR322 DNA with ethidium (left curve, large filled circles), **1** (middle curve, small filled circles), and **2** (lower curve, open circles). Conditions were the same as for the linear DNA titrations.

nonbonded requirements; the overall S-shape that the molecule adopts (Figure 1) is likely to be close in energy to a U-shape conformation having the two amine groups pointing in the same direction.

Mode of Binding. Classical intercalators such as ethidium bromide cause significant increases in sonicated DNA viscosity and an increase, due to uncoiling, followed by a decrease, due to reverse coiling, in closed circular supercoiled DNA viscosity.[1-3] Titrations of linear and supercoiled DNA with **1** and **2** are shown in Figure 2 and are compared to results for ethidium. With both DNA samples, **2** behaves as expected for a groove-binding molecule while **1** behaves as an intercalator but does not increase DNA length and does not unwind DNA base pairs to the extent that ethidium does. The unwinding experiments for ethidium and **1** were conducted at a range of DNA concentrations and plotted

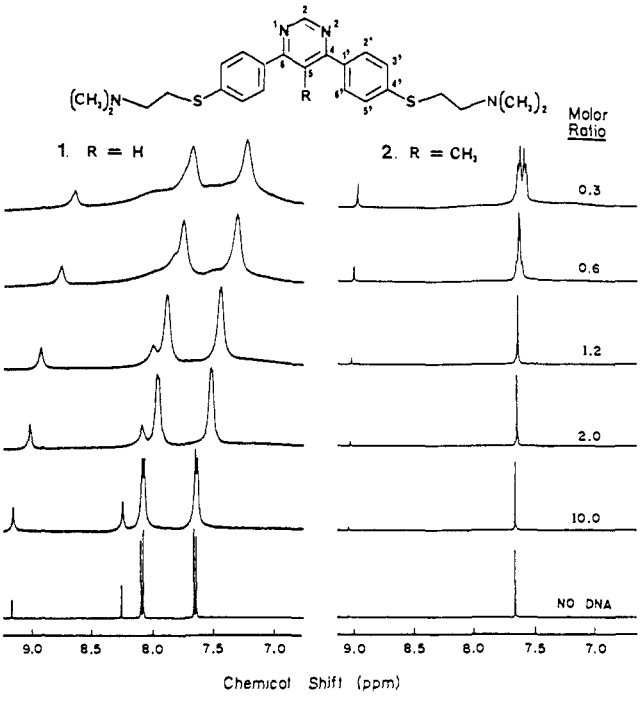

Figure 3. Spectra in the aromatic proton region for **1** (left) and **2** (right) at 1 mM concentration are shown as a function of the molar ratio (compound/base pair) of added DNA. Spectra were obtained at 65 °C on a Varian VXR 400 spectrometer (general conditions: 16 K data points, 4000-Hz spectral width, 2-s pulse repetition rate, 0.1-Hz line broadening). Samples (0.7 mL) in 99.96% D_2O (twice lyophilized from 99.8% D_2O) contained 0.015 M NaH_2PO_4, 0.1 mM EDTA, 0.1 M NaCl, pH = 7, and TSP as an internal reference.

by the Vinograd method.[1,2,17-19] With the value of 26° for the unwinding angle of ethidium as a standard, the unwinding angle of **1** is calculated to be only 8°. In the same way, the effective length increase in sonicated DNA produced by binding of **1**, calulated from the viscosity results of Figure 2A with the method of Cohen and Eisenberg,[20] is only approximately one-third of that produced by ethidium binding.

Flow dichroism studies[21,22] of a **1**–DNA complex resulted in a reduced dichroism of −0.129 at 260 nm and −0.082 at 330 nm in PIPES buffer with 0.2 M NaCl. The complex of **2** with DNA had essentially zero reduced dichroism (+0.002) at 305 nm, the maximum wavelength of the complex, under all conditions investigated. The flow dichroism signal of the complex of **1** with DNA was significantly reduced at all wavelengths in PIPES without added NaCl, suggesting that alternative binding modes become available to **1** at low ionic strength. With the phenanthridinium ring of ethidium, the reduced dichroism under these conditions is actually slightly larger than that obtained with the DNA pairs.

^1H NMR spectra in the aromatic region are shown for **1** and **2** in Figure 3 (bottom). Significant differences in the chemical shifts of equivalent protons on **1** and **2** occur, which are expected based on the larger twist of the phenyl–pyrimidine planes of **2** relative to **1**.[23] The large differences in the chemical shifts for

(17) Revet, B.; Schmir, M.; Vinograd, J. *Nature (London), New. Biol.* **1971**, *229*, 10–14.
(18) (a) Jones, R. L.; Lanier, A. C.; Keel, R. A.; Wilson, W. D. *Nucleic Acids Res.* **1980**, *8*, 1613–1624. (b) Kitchen, S. E.; Wang, Y. H.; Baumstark, A. L.; Wilson, W. D.; Boykin, D. W. *J. Med. Chem.* **1985**, *28*, 940–944.
(19) (a) Wang, J. C. *J. Mol. Biol.* **1974**, *89*, 783–801. (b) Pulleyblank, D. E.; Morgan, A. R. *J. Mol. Biol.* **1975**, *91*, 1–13.
(20) Cohen, G.; Eisenberg, H. *Biopolymers* **1969**, *8*, 45–69.
(21) Bloomfield, V. A.; Crothers, D. M.; Tinoco, I. *Physical Chemistry of Nucleic Acids*; Harper and Row: New York, 1974.
(22) (a) Banville, D. L.; Wilson, W. D.; Marzilli, L. G. *Inorg. Chem.* **1985**, *24*, 2479–2483. (b) Banville, D. B.; Marzilli, L. G.; Strickland, J. A.; Wilson, W. D. *Biopolymers* **1986**, *25*, 1837–1858.
(23) (a) Thummel, R. P.; Jahng, Y. *J. Org. Chem.* **1987**, *52*, 73–78. (b) Thummel, R. P.; Decloitre, Y.; Lefoulon, F. *J. Heterocycl. Chem.* **1986**, *23*, 689–693 and references therein.

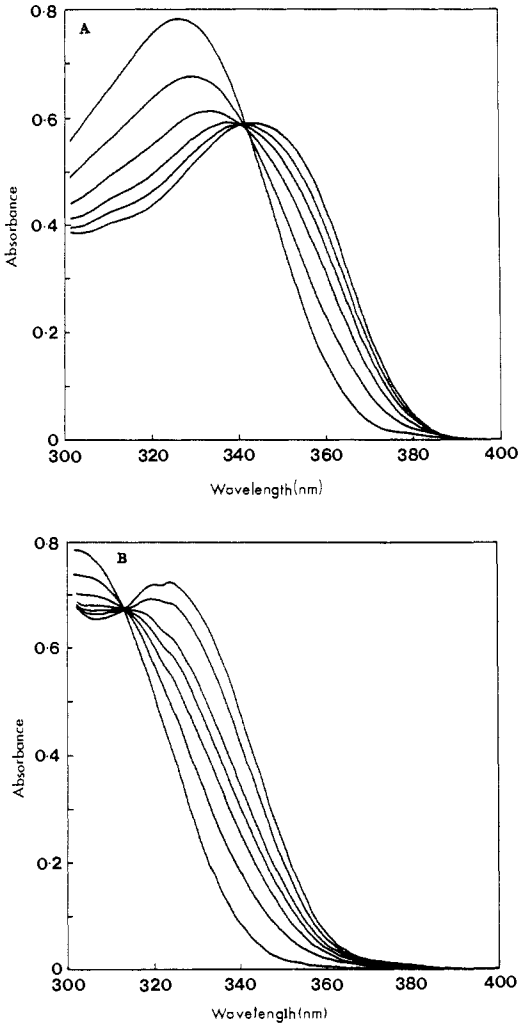

Figure 4. Spectral shifts for (A) **1** and (B) **2** on addition of calf thymus DNA. (A) The concentration of **1** was 2.5×10^{-5} and the DNA concentration in base-pair molarity for the curves of the figure increased as follows: (1) 0; (2) 1.6×10^{-5}; (3) 3.3×10^{-5}; (4) 4.8×10^{-5}; (5) 6.5×10^{-5}; (6) 8×10^{-5}. The top curve at 325 nm is for the free compound. (B) The concentration of **2** was 3.3×10^{-5} and the DNA concentration increased as follows: (1) 0; (2) 4×10^{-5}; (3) 8×10^{-5}; (4) 1.2×10^{-4}; (5) 1.6×10^{-4}; (6) 3.1×10^{-4}; (7) 6.2×10^{-4} M. The top curve at 302 nm is for the free compound. The cell path length in both titrations was 1 cm.

H2′(6′) and H3′(5′) in **1** are largely the result of the ring current effect of the pyrimidine ring on the adjacent protons H2′(6′) of the phenyl groups in the conformation with low torsional angles. As a result, the H2′(6′) protons are shifted downfield by approximately 0.5 ppm relative to the H3′(6′) protons of **1** and relative to all phenyl protons of **2**.

Addition of DNA results in signal broadening and upfield shifts of the aromatic protons of **1** as expected for an intercalation binding mode.[24] The shifts for the aromatic protons are −0.4 to −0.5 ppm at the 0.3 ratio (Figure 3) (H2, −0.51 ppm; H5, −0.48 ppm; H2′, H3′, H5′, and H6′, −0.41 ppm). All side-chain protons shift 0.03 ppm or less over the same titration range. The proton signals shift as single bands during the titration, indicating that free and bound **1** are in fast exchange under the conditions of these experiments.

In free **2** all phenyl protons have the same chemical shift, and, thus, no coupling can be detected. As DNA is added, one proton signal moves slightly upfield, and, by the 0.3 ratio, the signals for the *o*- and *m*-phenyl protons are resolved and coupling can be

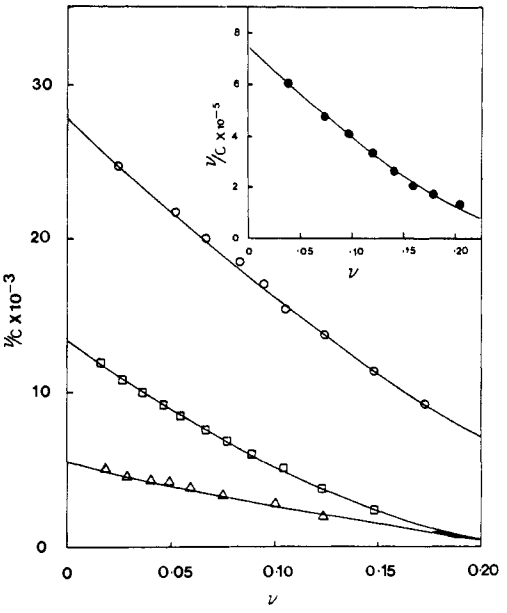

Figure 5. Scatchard plots of the binding of **1** to calf thymus DNA at 25 °C in PIPES buffer at different ionic strengths: (●) no added NaCl; (○) 0.05 M NaCl; (□) 0.1 M NaCl; and (△) 0.15 M NaCl. Points in the figure are the data, and the solid lines are the best fits from the McGhee–von Hippel model.[25]

detected. This differential shift suggests that **2** must be inserted at least partially into a groove of DNA and experiences a small upfield shift due to the ring currents of DNA base pairs. All shifts, however, are −0.05 ppm or less, and the signals are much less broad than with **1** (Figure 3). As with **1**, the signals shift as a single band, indicating fast exchange between free and bound species under these conditions. In NMR experiments in H_2O, **1** caused a 0.5 ppm upfield shift of the DNA imino protons and a 0.2 ppm downfield shift of the DNA ^{31}P NMR signal (50 °C for ^1H, 60 °C for ^{31}P, and a ratio of 0.6 mol of **1**/base pair). Addition of **2** to DNA did not result in a significant shift for the DNA imino proton or ^{31}P signals under the same conditions.

Binding Strength and Specificity. The interaction of **1** and **2** with DNA was monitored by observing their UV spectra above 300 nm on addition of DNA (Figure 4). The long-wavelength UV maximum for **1** is at 325 nm ($\epsilon = 30\,800$ M^{-1} cm^{-1}) while the maximum is shifted to 302 nm ($\epsilon = 23\,800$ M^{-1} cm^{-1}) for **2**, in agreement with the significantly larger predicted twist and loss of long-range conjugation for **2** relative to **1**.[23] DNA induces shifts to longer wavelengths and hypochromicity in the spectra, indicating significant binding of both compounds (isosbestic points with calf thymus DNA at 340 nm for **1** and at 312 nm for **2**). With **1** both calf thymus DNA and poly[d(A-T)]·poly[d(A-T)] (poly[d(A-T)]$_2$) shift the maximum wavelength to 333 nm while poly[d(G-C)]·poly[d(G-C)] (poly[d(G-C)]$_2$) shifts the maximum to 328 nm. With **2** the shift with calf thymus DNA is to approximately 308 nm and with poly[d(A-T)]$_2$ to approximately 305 nm. With **2** the shift with poly[d(G-C)]$_2$ is actually to shorter wavelengths and is difficult to monitor exactly because of interference by DNA absorption near 300 nm and below.

With the extinction coefficients for **1** and **2** free and bound to the above three DNA samples, bound-ligand concentrations can be determined at a range of total ligand concentrations.[14,24b] Spectrophotometric binding results, for example, are shown for **1** at several salt concentrations in Figure 5 in the form of Scatchard plots. The points in the figure are experimental, and the lines are the nonlinear least-squares best fit values by the site exclusion model of McGhee and von Hippel.[25] The binding constants, K, determined by this method decrease significantly as the ionic strength is increased, but the number of base pairs per binding site, n, remains essentially constant at a value near 3. A plot of

(24) (a) Chandrasekaran, S.; Kusuma, S.; Boykin, D. W.; Wilson, W. D. *Magn. Reson. Chem.* **1986**, *24*, 630–637. (b) Wilson, W. D.; Wang, Y. H.; Kusuma, S.; Chandrasekaran, S.; Yang, N. C.; Boykin, D. W. *J. Am. Chem. Soc.* **1985**, *107*, 4989–4995.

(25) McGhee, J. D.; von Hippel, P. H. *J. Mol. Biol.* **1974**, *86*, 469–489.

Table II. Results of Molecular Mechanics Calculations for Compound 1 and the Hexamer d(TACGTA)[a]

	E(complex)	E(native drug)	E(B-form hexamer)	δE(binding)	E(perturbed hexamer)	E(perturbed drug)	δE(drug)	δE(DNA)
model A	-283.2	9.0	-271.8	-20.4	-214.1	25.5	16.5	57.8
model B	-273.4	9.0	-271.8	-10.6	-245.4	5.0	-4.0	26.4

[a] Energies are in kilocalories per mole. δE(binding) = E(complex) - [E(B-form hexamer) + E(drug)]. δE(drug) is the change in energy of the drug for the energy-refined crystallographic conformation compared to that in the intercalated complex. δE(DNA) is the destabilization energy of the hexamer: E(perturbed hexamer) - E(native hexamer).

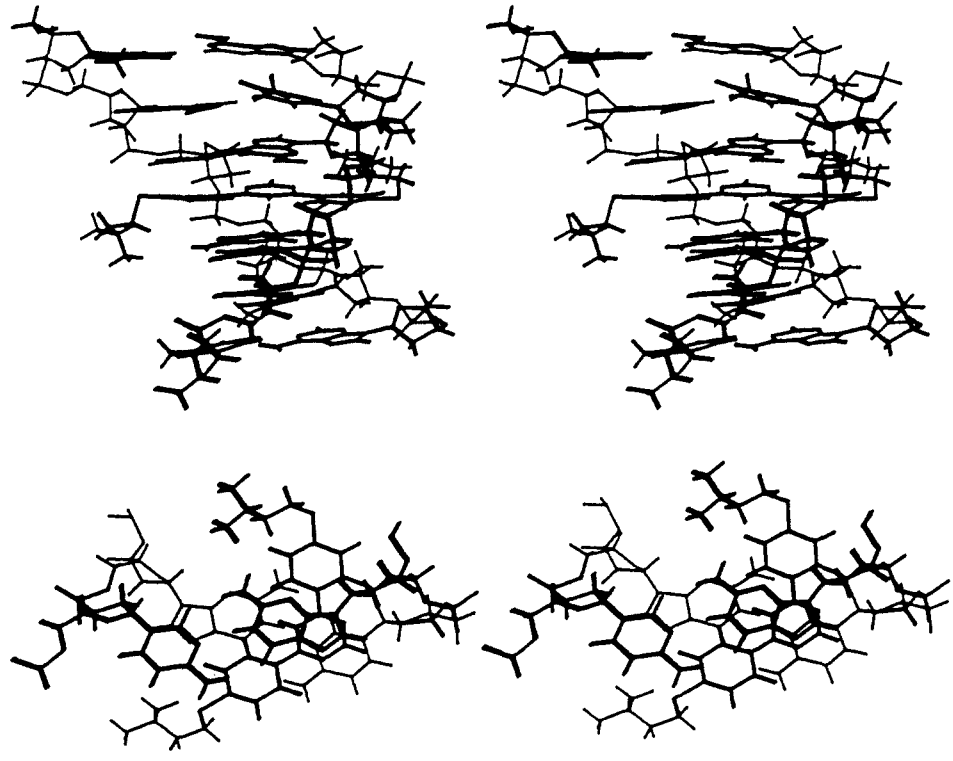

Figure 6. Stereoviews of model A with the side chains of 1 in both the major and minor grooves: (top) views perpendicular to the helix axis (the side chain on the left side of the model is in the major groove of the complex); (bottom) view down the helix axis (the base pair above 1 has dark lines, and the base pair below has thin lines) other base pairs have been eliminated for clarity. The major groove is at the bottom of the lower structures.

log K versus -log [Na^+] has a slope of 1.8, indicating that both alkyl amino groups of 1 can form ion pairs with phosphate groups in the DNA complex.[26,27] The binding constant of 2 is significantly less (27.7×10^3 M^{-1} at the lowest ionic strength of Figure 5) and also decreases with increasing ionic strength. The binding constant of 2 was too low ($K < 2 \times 10^3$), above 0.05 M Na^+ for accurate determination.

In binding measurements with calf thymus DNA, poly[d(A-T)]$_2$ and poly[d(G-C)]$_2$, both 1 and 2 exhibited some A·T base-pair specificity. In PIPES 10 buffer, for example, 1 has binding constants to poly[d(A-T)]$_2$, DNA, and poly[d(G-C)]$_2$ of 86, 13, and 7.2×10^3 M^{-1}, respectively. In PIPES 00 buffer 2 has binding constants of 73, 28, and 18×10^3 M^{-1} to the same three DNA samples. These results are somewhat unusual since intercalators are generally slightly G·C specific,[28] although exceptions are known.[24b] Outside binding molecules are typically A·T specific.[7]

Amplification Activity. The bleomycin-mediated digestion of DNA is enhanced (amplified) by some nonfused aromatic cation[8,9] compounds that distort the double helix. The DNA degradation in the absence and presence of amplifiers can conveniently be quantitated by monitoring decreases in DNA viscosity during the reaction.[9b,e] In a standard viscometric test,[9b] compound 1 caused increases of the apparent degradation rates by factors of 1.5 and 7.9 at molar ratios of compound to DNA base of 0.093 and 0.47, respectively. Under the same conditions the respective enhancement values for 2 were only 1.1 and 2.1.

Molecular Modeling. Two distinct low-energy intercalation positions for 1 were located (Table II) at the GC intercalation site of d(TACGTA) with molecular mechanics methods. Model A has 1 intercalated (Figure 6) so that the side chains are occupying both grooves. Stereoviews of the complex perpendicular (Figure 6A) and parallel to the helix long axis (Figure 6B) are shown. Model B has the ligand situated in the major groove of the DNA (Figure 7; views shown as in Figure 6), with the side chains stretched so as to interact with the anionic phosphodiester backbones, and has a δE(binding), which is approximately 10 kcal/mol higher than that for model A (Table II). An analogous complex for 1 in the minor groove was not feasible due to a large number of close contacts; the narrow width of the minor groove, therefore, inhibits binding of 1. The major groove binding in model B can be considered to be an intercalative one, since the three rings of 1 are partially stacked between base pairs (Figure 7B) although this is considerably less than for simpler intercalators such as proflavine.[29,30] Table II shows that the δE of the drug is negative, so that its conformation is stabilized on binding.

Discussion

Unwinding and extension of the DNA backbone in intercalation complexes results in length and viscosity increases in sonicated DNA, uncoiling and reverse coiling of superhelical DNA, and downfield shifts in DNA ^{31}P NMR spectra.[1-4] The stacking of

(26) Record, M. T., Jr.; Anderson, C. F.; Lohman, T. M. *Q. Rev. Biophys.* **1978**, *24*, 103-178.
(27) (a) Wilson, W. D.; Krishnamoorthy, C. R.; Wang, Y. H.; Smith, J. C. *Biopolymers* **1985**, *24*, 1941-1961. (b) Wilson, W. D.; Lopp, I. G. *Biopolymers* **1979**, *18*, 3025-3041.
(28) Müller, W.; Crothers, D. M. *Eur. J. Biochem.* **1975**, *54*, 267-277.
(29) Shieh, H.-S.; Berman, H. M.; Dabrow, M.; Neidle, S. *Nucleic Acids Res.* **1980**, *8*, 85-97.
(30) Islam, S. A.; Neidle, S. *Acta Crystallogr.* **1984**, *B40*, 424-429.

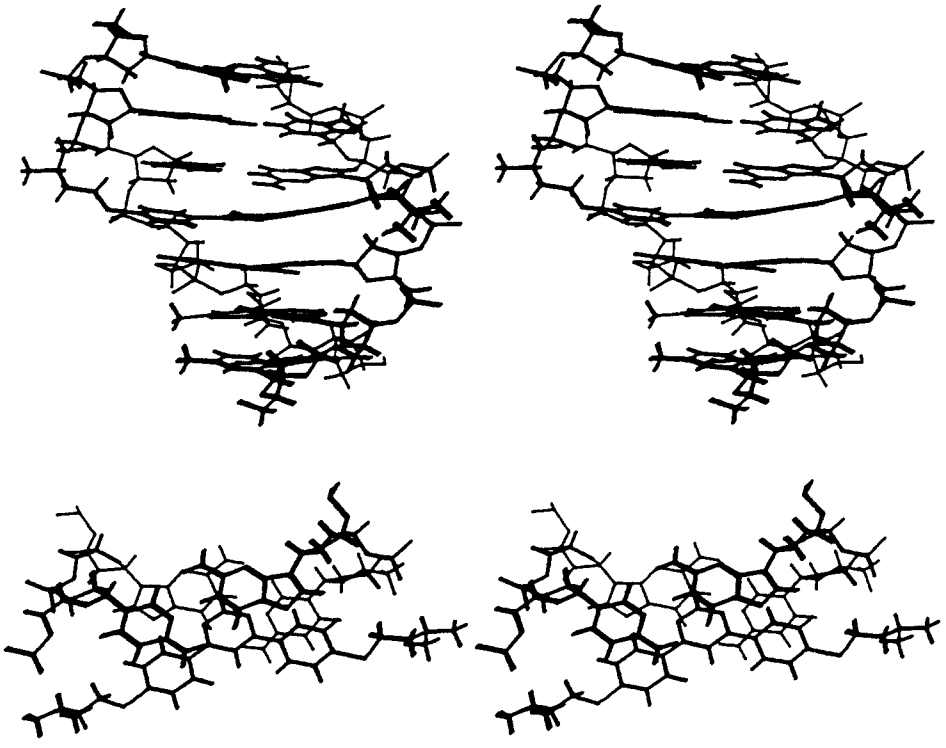

Figure 7. Stereoviews of model B with both side chains in the major groove: (top) view perpendicular to the helix axis and into the major groove of the complex; (bottom) view down the helix axis with the base pairs stacked as in Figure 6. The major groove is at the bottom of the lower structures.

base pairs with the aromatic ring system of an intercalator results in upfield shifts for DNA base and intercalator protons and a negative reduced dichroism.[1-4,9,24b] Analysis of the results presented above indicates that **1** forms a strong intercalation complex while **2** forms a groove-bound complex with DNA. These results demonstrate for the first time that a compound with significant twist in the equilibrium conformation in solution can bind to DNA with the twisted ring system intercalated. They also clearly demonstrate that there is a twist limit past which intercalation is no longer favorable relative to groove-binding interactions. Under the conditions of our experiments, the binding constant of **1** is similar to binding under the same conditions of strong intercalators such as ethidium and quinacrine, which have fused ring systems.[27a]

The aromatic rings of **1** are clearly twisted with respect to each other, and the conformation of **1** in the DNA complex is of considerable interest. It is known that the base pairs in DNA are twisted about their long axes (propeller twist),[12,13] and it seems possible that the twist of **1** may complement that of the base pairs. This would allow the bases to retain or enhance propeller twist to form a new type of intercalation complex. The alternative of stacking forces from the base pairs at the intercalation complex causing the three rings of **1** to assume a largely planar structure, as with the more usual fused ring intercalators, seems to us inherently less likely due to the severe steric clash of the H5 and H2′, H2″ (or H6′, H6″) protons in a planar conformation. Several of our experimental observations suggest that the DNA helix is more distorted, relative to the usual intercalation conformation, when **1** is bound.

First, the UV, spectral maximum of **1** should be sensitive to the twist angle of the three rings and should shift to longer wavelengths as the ring torsional angles are decreased.[23] There is an approximate 10-nm shift of the maximum to longer wavelengths, but this is not a large shift for an intercalator and, in fact, is not significantly greater than seen when **2** binds in the DNA grooves.

Second, the chemical shifts for the aromatic ring protons of **1** are quite sensitive to the twist angle of the three rings (compare spectra for **1** and **2** in Figure 3) and should exhibit marked differential shifts if the twist angle changes on intercalation. The shift observed for the 2′, 6′ protons, for example, should be significantly different from the shifts for the 3′, 5′ protons. In fact, the observed changes in chemical shifts are very similar when **1** binds to DNA. Classical intercalator stacking with the DNA bases usually results in a 0.8 ppm or greater upfield shift of intercalator aromatic protons,[24] but with **1** the shifts are only 0.4–0.5 ppm, suggesting that the contact with base pairs may not be as close as with the more common intercalators. These arguments must, however, be viewed as qualitative since there are competing effects on the spectral properties of **1** from the conformation of the compound itself and the local effects of the DNA intercalation site.

Third, the effect of **1** on DNA conformation appears quite different from the results seen with classical intercalators such as ethidium. The viscosity increase and unwinding angle on addition of **1** to DNA are significantly less than those with ethidium. Unwinding angles vary greatly with intercalator structure, but small relative increases in DNA viscosity in a titration with intercalators have been interpreted in terms of DNA bending.[2,31] The shifts of DNA imino proton and ^{31}P NMR signals on addition of **1** are only about half as much as those seen with intercalators such as ethidium and propidium.[32]

All of these results suggest that **1** intercalates with DNA, retains a significant amount of twist between the phenyl and pyrimidine rings, and causes a distortion of the DNA duplex at the intercalation site. With **2** the twist is too large for intercalation, and only groove binding is observed for this compound. At low ionic strengths the magnitude of the negative-reduced flow dichroism of DNA–**1** complexes is decreased, suggesting that groove binding may begin to compete with the intercalation binding mode. The A·T base-pair binding selectivity of **1** is opposite to the G·C selectivity usually observed with intercalators.[28] Since A·T base pairs with two hydrogen bonds are less stable than G·C base pairs, this selectivity agrees with the binding model involving DNA distortion at the intercalation site. It is interesting that compound **2**, which as a groove-binding molecule would be expected to favor binding to A·T base pairs, is actually less A·T specific than **1**.

(31) Gabbay, E. J.; Scofield, R. E.; Baxter, C. S. *J. Am. Chem. Soc.* **1973**, *95*, 7850–7857.
(32) Chandrasekaran, S.; Jones, R. L.; Wilson, W. D. *Biopolymers* **1985**, *24*, 1963–1979.

We have turned to molecular mechanics studies for more detailed ideas of possible structures of the **1**–DNA complex. A detailed search of intercalation complexes predicted that only models A and B (Table II, Figures 6 and 7) are possible stable intercalation conformations. Model A is analogous to that predicted by modeling for the anthracycline drug nogalamycin[33] and some anthraquinone ligands.[34] However, in these instances, this threaded-through, straddling mode is the only one possible in order for intercalation to occur. This is not the case with **1** since binding mode B is an alternative. On the basis of several considerations, we believe model B is the more feasible of the two since (a) straddling would involve base-pair hydrogen-bond disruption (the side-chains are too bulky to allow simple insertion through a 6.8 Å wide site), (b) the side chain in the minor groove would disrupt additional water, which, at least for some sequences, is more firmly bound in the minor groove, (c) intercalators that thread side chains through the helix show much slower binding kinetics than other similar intercalators[35,36] (NMR (Figure 2) and preliminary stopped-flow kinetics experiments with **1** indicate that its bound-state lifetime is quite short).

The binding constant of **2** is reduced relative to **1**. By increasing the twist of the three ring system, we have prevented intercalation but have not designed a strong groove-binding compound. The twist of **2** is too large to allow it to fit well into the narrow minor groove, and it probably binds weakly in the DNA major groove. We believe it binds, at least partially, in the groove rather than simply at the phosphate groups for four reasons: (i) It causes a slight increase in DNA viscosity whereas simple phosphate interactions generally slightly reduce DNA viscosity.[20] (ii and iii) Binding to DNA induces a slight upfield shift in the aromatic NMR signals of **2** and a UV spectral shift to longer wavelengths. Both of these effects suggest a weak interaction of **2** with the DNA bases.[2] (iv) The slight amplification of bleomycin degradation by **2** is consistent with a weak ineraction with the DNA bases.[9]

The suggestion that DNA can be fairly easily distorted by twisted intercalators such as **1** while maintaining a relatively high equilibrium constant for intercalation is quite interesting. We are synthesizing other series of unfused compounds to define more clearly the differential forces responsible for intercalation binding and to determine more exactly the maximum torsional twist that intercalating ring systems can have. High-resolution NMR studies of **1** with synthetic oligonucleotides and more detailed molecular modeling experiments are in progress to evaluate the fine structural features of the DNA complex.

Experimental Section

Materials. Buffers: PIPES buffer used in all experiments was 0.01 M PIPES, 10^{-3} M EDTA at pH = 7. Where desired, NaCl was added to increase the ionic strength.

***N,N*-Dimethyl-2-[(4′-bromophenyl)thio]ethylamine (3).** A solution of 2-dimethylaminoethyl chloride hydrochloride (19 g, 0.132 mol) in water (75 mL) was added to a solution of *p*-bromobenzenethiol (25 g, 0.132 mol) and sodium hydroxide (12 g, 0.3 mol) in aqueous ethanol (1:1, 200 mL). The mixture was stirred at 80 °C for 1 h and then extracted with ether (3 × 100 mL). The ether was stirred with hydrochloric acid (2 N, 70 mL). The aqueous layer was made alkaline and extracted with ether (3 × 100 mL). The extract was dried (Na_2SO_4), concentrated, and distilled in a Kugelrohr [120 °C (0.15 mmHg)] to give 33.0 g (96%) of **3** as a colorless oil: ^{1}H NMR ($CDCl_3$) δ 2.27 (s, 6 H), 2.54 (t, J = 7.2 Hz, 2 H), 3.01 (t, J = 7.2 Hz, 2 H), 7.20 (d, J = 8.2 Hz, 2 H), 7.39 (d, J = 8.2 Hz, 2 H). Anal. ($C_{10}H_{14}BrNS$) C, H.

***N,N*-Dimethyl-2-[[4′-(pyrimidin-4″-yl)phenyl]thio]ethylamine (5).** A solution of **3** (3.9 g, 15 mmol) in ether (75 mL) was treated dropwise at −35 °C with *n*-butyllithium in hexanes (2.6 M, 5.8 mL, 15.1 mmol), and the resultant mixture was stirred at −35 °C for 1 h. A solution of pyrimidine (1.2 g, 15 mmol) in ether (3 mL) was added with stirring at −50 °C. The mixture was stirred at −50 °C for 30 min, quenched at 0 °C with water (0.5 mL) in THF (5 mL), and then treated with a solution of 2,3-dichloro-5,6-dicyanobenzoquinone (3.4 g, 15 mmol) in THF (50 mL) and stirred at 25 °C for 1 h. Treatment with aqueous sodium hydroxide (10%, 50 mL) was followed by extraction with ether (4 × 50 mL). Chromatography on silica gel [hexanes/dichloromethane/triethylamine (45:45:10)] and then crystallization from hexanes gave 1.55 g (40%) of **5**: mp 78–79 °C; ^{1}H NMR ($CDCl_3$) δ 2.30 (s, 6 H), 2.62 (t, J = 7.2 Hz, 2 H), 3.13 (t, J = 7.2 Hz, 2 H), 7.42 (d, J = 8.2 Hz, 2 H), 7.68 (d, J = 5.5 Hz, 1 H), 8.02 (d, J = 8.2 Hz, 2 H), 8.75 (d, J = 5.5 Hz, 1 H), 9.24 (s, 1 H). Anal. ($C_{14}H_{17}N_3S$) C, H, N.

***N,N*-Dimethyl-2-[[4′-(5″-methylpyrimidin-4″-yl)phenyl]thio]ethylamine (6).** Substitution of 5-methylpyrimidine (1.41 g, 15 mmol) for pyrimidine in the procedure described above gave **6** (2.09 g, 51%) as an oil: ^{1}H NMR ($CDCl_3$) δ 2.29 (s, 6 H), 2.38 (s, 3 H), 2.60 (t, J = 7.2 Hz, 2 H), 3.05 (t, J = 7.2 Hz, 2 H), 7.38 (d, J = 8.2 Hz, 2 H), 7.52 (d, J = 8.2 Hz, 2 H), 8.54 (s, 1 H), 9.03 (s, 1 H). Anal. ($C_{15}H_{19}N_3S$) C, H, N.

4,6-Bis[4′-[[2″-(dimethylamino)ethyl]thio]phenyl]pyrimidine (1). Substitution of **5** (0.68 g, 2.62 mmol) for pyrimidine or 5-methylpyrimidine in the procedures described above, with the same molar ratios of other reagents, gave 0.77 g (67%) of **1**, mp 70–72 °C. ^{1}H NMR: see Figure 3. Anal. ($C_{24}H_{30}N_4S_2$) C, H, N.

4,6-Bis[4′-[[2″-(dimethylamino)ethyl]thio]phenyl]-5-methylpyrimidine (2). An analogous treatment of **6** (1.18 g, 4.32 mmol) gave 0.63 g (32% of **2** as an oil. Treatment of a warm solution of **2** in ethanol (10 mL) with hydrobromic acid (48%, 0.5 mL), followed by cooling, gave a dihydrobromide, mp 272–274 °C. ^{1}H NMR: see Figure 3. Anal. ($C_{25}H_{32}N_4S_2 \cdot 2HBr$) C, H, N.

Preparation of Plasmid pBR 322. *Escherichia coli* strain K336 was grown in Luria–Bertani media with 25 μg/L ampicillin and amplified with 100 mg/L chloroamphenicol.[37] After the bacteria were harvested, the cleared lysate was prepared by lysis with lysozyme and 1% sodium dodecyl sulfate in 0.2 N NaOH solution.[38] The suspension was centrifuged at 38 000 rpm for 45 min, and the supernatant was decanted and treated with poly(ethylene glycol). The precipitate was collected by centrifugation and resuspended in a Tris buffer solution (10 mM Tris/HCl, 1 mM EDTA, pH = 7.0). The suspension was brought to a urea concentration of 7 M, incubated at 40 °C for 15 min, and filtered through an 0.45-μm filter. The plasmid was obtained by an HPLC separation of the filtrate on a 10 × 125 mm Nucleogen DEAE4000-7 column (5 M urea, 20 mM K_3PO_4, pH = 6.9, linear increasing concentration of KCl from 0.3 to 1.5 M over 40 min with a flow rate of 1 mL/min) followed by dialysis in PIPES buffer at 4 °C. Electrophoresis showed more than 95% of supercoiled form I, less than 5% of circular form II, and absence of linear form III. When stored with 1 drop of chloroform at 4 °C, the sample did not significantly change its composition over a period of 1 month.

Methods. Procedures for viscometric titrations,[18] flow dichroism,[22] spectrophotometric binding,[27] and NMR measurements[24] have been recently presented.

Crystallography. Prismatic crystals of **1** were obtained by slow evaporation of a 10:1 ethanol/water solution. Cell dimensions were obtained by least-squares refinement of 25 θ values measured on an Enraf–Nonius CAD4 diffractometer. They are the following: a = 6.296 (1), b = 11.855 (2), c = 18.463 (2) Å; α = 84.49 (1), β = 85.65 (1), γ = 75.96 (1)°. The calculated density for two molecules of $C_{24}H_{30}N_4S_2Br_2$ in this unit cell of volume 1328.9 Å^2 is 1.496 g cm^{-1}. The provisional assignment of the space group as $P1$, with Z = 2, was confirmed by the successful structure analysis and refinement in this space group. The absorption coefficient is 54.9 cm^{-1}. Intensity data were collected on the diffractometer with Cu Kα radiation on a small crystal of dimensions 0.15 × 0.10 × 0.06 mm, to a limit of θ = 70° with an ω–2θ scan technique and a maximum scan time of 90 s/reflection. A total of 5067 reflections were measured, of which 3575 had $I \geq 3\sigma$ for the 4886 unique reflections. A periodic check on three standard reflections during the data collection did not indicate any significant radiation decay.

The structure was solved by direct methods with the MULTAN program,[39] as implemented in the SDP crystallographic program system[40] and run on a VAX computer. The most consistent E-map revealed the positions of the bromine atoms and some of the other non-hydrogen atoms. The remainder were found in difference Fourier syntheses.

(33) Collier, D. A.; Neidle, S.; Brown, J. R. *Biochem. Pharmacol.* **1984**, *33*, 2877–2880.
(34) Islam, S. A.; Neidle, S.; Gandecha, B. M.; Partridge, M.; Patterson, L. H.; Brown, J. R. *J. Med. Chem.* **1985**, *28*, 857–864.
(35) Yen, S. F.; Gabbay, E. G.; Wilson, W. D. *Biochemistry* **1982**, *21*, 2070–2076.
(36) Krishnamoorthy, C. R.; Yen, S. F.; Smith, J. C.; Lown, J. W.; Wilson, W. D. *Biochemistry* **1986**, *25*, 5933–5940.
(37) Hillen, W.; Klein, R. D.; Wells, R. D. *Biochemistry* **1981**, *20*, 3748–3756.
(38) Garger, S. J.; Griffith, O. M.; Grill, L. K. *Biochem. Biophys. Res. Commun.* **1983**, *117*, 835–842.
(39) Main, P.; Fiske, S. J.; Hull, S. E.; Lessinger, L.; Germain, G.; Declercq, J.-P.; Woolfson, M. M. *Multan 82. A System of Computer Programs for the Automatic Solution of Crystal Structures from X-ray Diffraction Data*; University of York: England, 1982.
(40) *The SDP Structure Determination Package*; Enraf-Nonius: Delft, Holland, 1986.

Refinement was carried out by full-matrix least-squares techniques, with all non-hydrogen atoms being assigned anisotropic temperature factors. The positions of some hydrogen atoms were determined from difference Fourier maps; those for others were generated by standard geometric considerations. All hydrogen atoms were assigned an isotropic temperature factor of 5.0 Å^2. The positional parameters of those attached to the rings were included in the least squares. An empirical adsorption correction[41] was applied to the data. Weights used were of the type $w = 1/[\sigma^2(F_o + 0.04F^2)]$. Refinement converged at an unweighted R of 0.057 and an R_w of 0.073, where $R_w = [\sum w(|F_o| - |F_c|)^2/\sum|F_o|^2]^{1/2}$. The maximum shift/error was 0.02. The final difference Fourier showed maximum and minimum electron densities of +0.4e and −0.36e, respectively. Tables of anisotropic thermal parameters, hydrogen atom positions, and structure factors have been deposited as supplementary material.

Molecular Modeling. Interactive computer graphics techniques were used to dock the structure of compound **1** into a model of duplex DNA with an intercalation site. This model is of the alternating hexanucleotide sequence d(TACGTA) and has an intercalation site between the central CG base pairs. It has been constructed by means of least-squares fitting of B-DNA residues to both ends of the CG dinucleoside geometry found in its crystalline complex with proflavine, followed by energy minimization. The docking of compound **1** was performed on a Silicon Graphics IRIS work station with the GEMINI molecular graphics program.[42] The docking process was accompanied by alterations in the conformation of the ligand's side chains. Positions of potential low energy, as judged by maximum stacking of the rings of **1** with base pairs together with minimal repulsive close contacts, were located and subjected to molecular mechanics conjugate gradients full-geometry minimization. The force field used is of the form $E(\text{total}) = E(\text{nonbonded}) + E(\text{electrostatic}) + E(\text{torsion}) + E(\text{angle}) + E(\text{bond})$. The parameter set used for the DNA was the all-atom representation published by Kollman et al.[43] Partial charges for the cation of **1** were obtained by CNDO/2 calculations. Geometry was taken directly from the X-ray analysis reported here. Force constants and torsional potentials for the bond and atom types of **1** not represented in the published tables,[43] especially for aliphatic C–S and N–C, were assigned according to established procedures.[43,44] A distance-dependent dielectric constant was used, of the form $\epsilon = 4r_{ij}$. Convergence was judged to have been achieved during the energy refinement when the rms value of the first derivative was less than 0.15.

Acknowledgment. This work was supported by NSF Grant DBM-8603566 (W.D.W.), a NATO Travel Award (W.D.W. and S.N.), American Cancer Society Grant CH383 (L.S.), the Greenwall Foundation, Inc., Research Corp. (L.S.), ACS-PRF Grant 18704 (L.S.), NIH Grant S07-RR07171 (W.D.W. and L.S.), and the Cancer Research Campaign (S.N.). The 400-MHz NMR spectrometer was obtained with partial support from a Departmental NSF Grant. We thank Professor David Boykin and Dr. T. C. Jenkins for helpful discussions and Dr. I. Haneef for supplying us with his molecular mechanics program.

Registry No. **1**, 117269-54-2; **2**, 117308-21-1; **3**, 90944-65-3; **5**, 117269-55-3; **6**, 117269-56-4; d(TACGTA), 100443-41-2; pyrimidine, 289-95-2; 5-methylpyrimidine, 2036-41-1.

Supplementary Material Available: Tables of hydrogen atom positions and anisotropic thermal parameters (3 pages); listing of observed and calculated structure factors (18 pages). Ordering information is given on any current masthead page.

(41) Walker, N.; Stuart, D. *Acta Crystallogr.* **1983**, *A34*, 1518–166.
(42) *The GEMINI Molecular Graphics Package*; Institute of Cancer Research: Sutton, U.K., 1988.
(43) Weiner, S. J.; Kollman, P. A.; Nguyen, D. T.; Case, D. A. *J. Comput. Chem.* **1986**, *7*, 230–252.
(44) Abraham, Z. H. L.; Agbandje, M.; Neidle, S., to be submitted for publication.

Time-Resolved Observation of Excitation Hopping between Two Identical Chromophores Attached to Both Ends of Alkanes

Tomiki Ikeda,*,† Bong Lee,† Seiji Kurihara,† Shigeo Tazuke,*,† Shinzaburo Ito,‡ and Masahide Yamamoto‡

Contribution from the Photochemical Process Division, Research Laboratory of Resources Utilization, Tokyo Institute of Technology, 4259 Nagatsuta, Midori-ku, Yokohama 227, and Department of Polymer Chemistry, Kyoto University, Kyoto 606, Japan.
Received October 13, 1987

Abstract: Excitation hopping between two identical chromophores has been directly observed by time-resolved fluorescence anisotropy ($r(t)$) measurements with the aid of a picosecond time-correlated single-photon counting system (fwhm 80 ps). In order to explore the excitation hopping behavior *in purely isolated two identical chromophoric systems*, we used α,ω-bis(2-naphthyl)-*n*-alkanes, Nap$(CH_2)_n$Nap (N*n*), where n = 3, 5, 7, and 12, as well as 2-ethylnaphthalene (EN) as a model compound. We show that $r(t)$ for EN does not change with time while $r(t)$ for N*n* decays with time, depending on n, and the initial decay of $r(t)$ becomes faster with decreasing n. Our results clearly indicate that excitation hopping takes place between the two naphthyl moieties attached to both ends of the alkyl chain. Theoretical treatment assuming forward and backward excitation hopping between the two naphthyl moieties has been carried out on the basis of the conformational analysis of N*n*'s, which manifested the distribution function of interchromophore distance and mutual orientation of the two naphthyl moieties. Results of the theoretical treatment have shown to account fairly well for the experimentally observed anisotropy decays.

Electronic excitation transport in molecular aggregate systems has become an area of challenge from both theoretical[1-3] and experimental[4-10] points of view. Since the excitation transport is essentially a phenomenon occurring in a pair of chromophores, the simplest case for the excitation transport in the molecular aggregate systems may be a bichromophoric system. Excitation transport between two nonidentical chromophores was easily

† Tokyo Institute of Technology.
‡ Kyoto University.

(1) (a) Pearlstein, R. M. *J. Chem. Phys.* **1972**, *56*, 2431. (b) Hemenger, R. P.; Pearlstein, R. M. *Ibid.* **1973**, *59*, 4064. (c) Haan, S. W.; Zwanzig, R. *Ibid.* **1978**, *68*, 1879. (d) Blumen, A.; Manz, J. *Ibid.* **1979**, *71*, 4694. (e) Godzik, K.; Jortner, J. *Ibid.* **1980**, *72*, 4471. (f) Blumen, A.; Klafter, J.; Silbey, R. *Ibid.* **1980**, *72*, 5320.

0002-7863/88/1510-8299$01.50/0